Cancer Gene Therapy (2012) **19,** 420 – 430

www.nature.com/cgt

ORIGINAL ARTICLE

Interferon-β lipofection II. Mechanisms involved in cell death and bystander effect induced by cationic lipid-mediated interferon-β gene transfer to human tumor cells

MS Villaverde, ML Gil-Cardeza, GC Glikin and LME Finocchiaro

We evaluated the cytotoxic effects (apoptosis, necrosis and early senescence) of human interferon-β (hIFNβ) gene lipofection. The cytotoxicity of hIFNβ gene lipofection resulted equivalent to that of the corresponding addition of the recombinant protein (rhIFNβ) on human tumor cell lines derived from Ewing's sarcoma (EW7 and COH) and colon (HT-29) carcinomas. However, it was stronger than rhIFNβ on melanoma (M8) and breast adenocarcinoma (MCF7). To reveal the mechanisms involved in these differences, we compared the effects of hIFNβ gene and rhIFNβ protein on EW7 and M8 (sensitive and resistant to rhIFNβ protein, respectively). Lipofection with hIFNβ gene caused a mitochondrial potential decrease simultaneous with an increase of oxidative stress in both cell lines. However, rhIFNβ protein displayed the same pattern of response only in EW7-sensitive cell line. The great bystander effect of the hIFNβ gene lipofection, involving the production of reactive oxygen species, would be among the main causes of its success. In EW7, this effect killed >60% of EW7 cell population, even though only 1% of cells were expressing the transgene. As hIFNβ gene was effective even in the rhIFNβ protein-resistant M8 cell line and in a way not limited by low lipofection efficiency, these results strongly support the clinical potential of this approach.

Cancer Gene Therapy (2012) **19,** 420–430; doi:10.1038/cgt.2012.19; published online 4 May 2012

Keywords: apoptosis; Ewing's sarcoma; interferon-β; lipofection; melanoma; reactive oxygen species

INTRODUCTION

Interferons (IFNs) are well known for both their *in vitro* and *in vivo* antiproliferative effect and immunomodulatory activity,[1,2] and they were the first cytokines to be applied clinically in human cancer.[3,4] Despite the demonstrated clinical effectiveness, the treatment with IFNα/β is associated with substantial systemic toxicity that worsens the patient's quality of life and often prejudices the therapy completion (~25% of the treated patients).[5]

The antiproliferative effect, however, relies on IFNβ concentrations that cannot be achieved by systemic protein administration because of toxicity, an extremely short half-life in the blood stream and rapid protein clearance. Pharmacokinetic studies indicate that the limited performance of IFNβ in cancer trials may have been caused by insufficient or lack of sustained delivery of the protein to the tumor site.[6] A continuous, low-level delivery of IFN might avoid its toxicity while maintaining, and probably improving, its antitumor efficacy. This type of pharmacokinetics could be achieved by a gene therapy-mediated approach. Thus, gene transfer would allow taking advantage of IFNα/β effectiveness without undesirable side effects.

Even though murine IFNβ adenoviral gene transfer was successfully applied for murine colorectal cancer liver metastases in immune-competent BALB/c mice,[7] the use of viral vectors carrying IFNα/β, cytokines that trigger antiviral responses, does not seem to be the best choice *a priori*. Both innate and acquired immunity toward adenovirus were described, a situation even more sensitive when the treatment should be repeated to reach a significant clinical outcome. In the case of a clinical trial for mesothelioma,[8] neutralizing antibodies against recombinant adenoviral particles carrying human hIFNβ (hIFNβ) gene prevented further rounds of transduction. Whereas safety and feasibility of the treatment were assessed, the clinical benefits resulted still poor. In this scenario, nonviral vectors carrying IFNα/β would not be limited by such constraints, as it was already proposed.[3] Cationic liposomes allowed multiple *in vivo* administrations of plasmids carrying therapeutic genes,[9] sometimes achieving long-term survival rate.[10,11] In the case of human glioma, the preliminary clinical effects obtained with adenoviral vectors[12] do not seem more encouraging than those obtained with liposomal vectors.[13]

Because local nonviral gene therapy has the potential to overcome the above-mentioned limitations, one of the aims of this study was to evaluate the *in vitro* antitumor activity of hIFNβ gene therapy compared with rhIFNβ protein in Ewing's sarcoma (ES) and other human tumor models. This proposal was based on: (1) our previous encouraging clinical data from veterinary soft tissue sarcoma patients[11] and (2) the demonstration that recombinant human IFNα and IFNβ inhibited the *in vivo* growth of established ES xenografts generated by the same cell lines used by us (EW7, COH).[14] The study of the mechanisms achieving to cell death and bystander effect induced by hIFNβ gene lipofection, probably involving reactive oxygen species, may provide a deeper insight on the action of this approach for gene therapy.

MATERIALS AND METHODS

Cell cultures

Human ES (EW7 and COH),[14] melanoma (M8),[15] mammary carcinoma (MCF7, ATCC, Manassas, VA, no. HTB-22) and colorectal adenocarcinoma

Unidad de Transferencia Genética, Instituto de Oncología 'Ángel H. Roffo', Universidad de Buenos Aires, Buenos Aires, Argentina. Correspondence: Dr LME Finocchiaro, Unidad de Transferencia Genética, Instituto de Oncología 'A. H. Roffo' – UBA, Av. San Martín 5481, 1417 Buenos Aires, Argentina.
E-mails: gglikin@bg.fcen.uba.ar and finolili@hotmail.com
Received 11 October 2011; revised 13 March 2012; accepted 13 March 2012; published online 4 May 2012

(HT-29, ATCC no. HTB-38) cells were cultured at 37 °C in a humidified atmosphere of 95% air and 5% CO_2 with Dulbecco's modified Eagle's medium (DMEM)/F12 medium (Invitrogen, Carlsbad, CA) containing 10% fetal bovine serum (Invitrogen), 10 mM HEPES (pH 7.4) and antibiotics. Serial passages were done by trypsinization (0.25% trypsin and 0.02% EDTA in phosphate-buffered saline (PBS)) of subconfluent monolayers.

Plasmids

Plasmids psCMVβ and psCMV-hIFNβ were built replacing the HSV thymidine kinase gene of psCMV*tk*[10] by *Escherichia coli* β-galactosidase (βgal)[16] and hIFNβ genes, respectively. Plasmids were amplified in *E. coli* DH5α (Invitrogen), grown in LB medium containing 100 μg ml^{-1} neomycin and purified by ion-exchange chromatography (Qiagen, Valencia, CA).

Liposome preparation and *in vitro* lipofection

DC-Chol (3β[*N*-(*N*′,*N*′-dimethylaminoethane)-carbamoyl cholesterol) and DMRIE (1,2-dimyristyloxypropyl-3-dimethyl-hydroxyethilammonium bromide) were synthesized and kindly provided by BioSidus (Buenos Aires, Argentina). DOPE (1,2-dioleoyl-*sn*-glycero-3-phosphatidyl ethanolamine) was purchased from Sigma (St Louis, MO). Liposomes were prepared at lipid/co-lipid molar ratios of 3:2 (DC-Chol:DOPE) or 1:1 (DMRIE:DOPE) by sonication as described.[16] Optimal lipid mixtures were determined for every cell line. Cultured cells at a density of 5×10^4 cells per cm^2 (~40% confluence) were exposed to lipoplexes (1 μl liposomes per cm^2 and 0.5 μg DNA per cm^2) during 4–6 h.

βgal staining

To measure gene transfer efficiency, psCMVβ-lipofected cells were trypsinized, fixed in suspension, stained with 5-bromo-4-chloro-3-indolyl β-D-galactopyranoside (X-GAL, Sigma) and counted using an inverted phase contrast microscope.[16]

Sensitivity to hIFNβ assay

At 24 h after lipofection, transiently hIFNβ- or βgal-expressing cells, were seeded on regular plates (5×10^4 cells per ml). Alternatively, nonlipofected cultured cells were treated with recombinant human IFN-α2b (Bioferon) or IFN-β2a (Blastoferon) kindly provided by BioSidus at the indicated concentrations. After 5 days of incubation, cell viability was quantified using a colorimetric CellTiter 96 Aqueous Non radioactive MTS Cell Proliferation Assay according to the manufacturer's instructions (Promega, Madison, WI). The percentage of cell survival was calculated from the ratio of the absorbances between lipofected and untreated control cells.

Flow cytometry cell cycle analysis

Untreated cells or both hIFNβ- or βgal-expressing cells were trypsinized, fixed in 70% (v/v) ethanol at −20 °C for 1 h, treated with RNase, stained with 10 μg ml^{-1} propidium iodide for 30 min, and subjected to single-channel flow cytometry on a Becton Dickinson FACScan (Franklin Lakes, NJ), with collection and analysis of data performed using Becton Dickinson CELLQuest software.[16]

p53 immunocytochemistry

Cells growing on glass slides were cultured for 48 h. Then, they were washed, fixed with cold acetone, dried, re-hydrated and incubated with primary antibody anti-p53, 1:500 (Santa Cruz Biotechnology, Santa Cruz, CA) overnight at 4 °C. After rinsing, cells were incubated with a 1:200 dilution of fluorescein isothiocyanate anti-mouse IgG (Sigma) at room temperature for 2 h. Nuclei were stained with 2-(4-amidinophenyl)-6-indolecarbamidine dihydrochloride (DAPI, Sigma) diluted 1:2000. A Nikon Eclipse TE 2000-S fluorescence microscope with a Nikon Digital Sight DS-U2 camera (Nikon Corporation, Tokyo, Japan) was employed. Images were processed by Corel Draw Graphics Suite X5 (Corel Corporation, Ottawa, ON, Canada) software using overlay when indicated.

Western blot analysis

Treated cultured cells were harvested, rinsed with PBS and lysated (25 mg protein in ice-cold NP-40 lysis buffer), sonicated and clarified by centrifugation. Lysates were subjected to SDS-polyacrylamide gel electrophoresis and blotted onto Immobilon-P membranes (Millipore, Bedford, MA). The filter was incubated in a solution of 50 mM Tris-HCl (pH = 7.5), 150 mM NaCl, 0.05% Tween-20, 5% dried low-fat milk for 12 h and then probed with mouse monoclonal anti-p53 (described above) or anti-actin antibodies (Sigma) at a concentration of 0.25 and 1.5 mg ml^{-1} in Tris-buffered saline and Tween-20. Horseradish peroxidase-conjugated goat antimouse IgG (Sigma) was used as second antibody (1:1000 dilution) for 1 h. Western bands were quantified with ImageJ 1.45s (National Institutes of Health, Bethesda, MD) software.

DNA ladder assay

Total genomic DNA was isolated from untreated or both hIFNβ- or βgal-expressing EW7 cells by SDS/Proteinase K lysis followed by phenol/chloroform extraction and ethanol precipitation, and then incubated with RNase A and electrophoretically separated on 1.2. % agarose gels stained with ethidium bromide.

Senescence

Senescence-associated expression of βgal activity was determined as described.[17] In brief, untreated, treated with 3 consecutive daily pulses of 1000 or 10 000 IU ml^{-1} rhIFNβ or both hIFNβ- or βgal-expressing EW7 cells were trypsinized, fixed in suspension and incubated in acidic condition with X-GAL (Sigma), 0.12 mM $K_3Fe(CN)_6$, 0.12 mM $K_4Fe(CN)_6$, 1 mM $MgCl_2$ in PBS, pH 6.5, at 37 °C overnight. Then, blue cells were counted using an inverted phase contrast microscope.

Mitochondrial potential evaluation

Mitochondrial membrane potential was evaluated by simultaneous staining with MitoTracker Red CMXRos (Invitrogen)[18] and calcein-AM (Invitrogen).[19] Briefly, control (untreated), βgal and hIFNβ-lipofected cells were incubated with 0.1 μM final concentration of both probes (pH 7.4, PBS) for 20 min, washed with PBS and then incubated in fresh DMEM/F12 medium for 30 min. Whereas accumulation of MitoTracker Red CMXRos (red staining) demonstrates a conserved mitochondrial potential, calcein-AM (green staining) marks all viable cells. Fluorescent images were captured with the above-mentioned microscope.

Intracellular reactive oxygen species detection

Intracellular oxidants levels were detected by DHDCFDA (Invitrogen).[20] Control (untreated), βgal and hIFNβ-lipofected cells were incubated with 0.1 μM final concentration of DHDCFDA (DMEM/F12 without fetal bovine serum) for 20 min, washed with PBS and then incubated in normal culture conditions. Fluorescent images were captured with the above-mentioned microscope. The total number of cells was evaluated using an inverted phase contrast microscope.

Chromogenic detection of superoxides

As described,[21] 250 μM nitro blue tetrazolium salt (NBT) dissolved in 70% dimethyl formamide in the culture medium was added to untreated EW7 cells, treated with consecutive daily pulses of 3000 IU ml^{-1} rhIFNβ or lipofected with hIFNβ or βgal genes cells for 6 h. When reacting with superoxide, NBT forms a water-insoluble blue formazan. Cells were then incubated for 20 min in a solution of 20% SDS and 50% dimethylformamide and detached from 24-well plates with a rubber policeman. The cell solution was boiled for 1 min to dissolve formazan crystals. After cell debris removal by brief spin down, absorbance was read at 570 nm.

Measurement of hydroperoxide (ROOH) concentrations in culture media

The concentration of H_2O_2 in the culture medium was measured by the Fe^{2+} oxidation-xylenol orange method[22] as follows: 100 μl medium of untreated or both hIFNβ- or βgal-expressing EW7 cells was mixed with

100 µl reaction solution containing 250 µM $[NH_4]_2[Fe][SO_4]_2 \cdot 6H_2O$, 50 mM H_2SO_4, 200 mM sorbitol and 2 mM xylenol orange, and incubated at room temperature for 45 min and absorbance was read at 595 nm.

Cellular antioxidant capacity assay

The determination of the antioxidant capacity of cells was adapted from the previously described luminol test.[23] Briefly, a PBS solution of 1×10^6 ml cells of control (untreated), βgal- and hIFNβ-lipofected cells was incubated with 0.1 µM luminol final concentration and 1 mM H_2O_2. The chemoluminescence of oxidized luminol was evaluated immediately, every 20 s, 25 times. Results were expressed as percentages of the values obtained for untreated cells (100%; $n = 4$).

Addition of exogenous antioxidant enzymes

After βgal or hIFNβ gene lipofection or the addition of 1000 or 3000 IU ml^{-1} of rhIFNβ, cell culture medium was supplemented with 100 IU ml^{-1} superoxide dismutase (SOD) or 1000 IU ml^{-1} catalase (CAT) or a combination of both antioxidant enzymes.

Supernatant cytotoxicity

The supernatants of control (untreated), βgal- and hIFNβ-lipofected cells were collected (48 h after lipofection), filtered (0.22 µm) and incubated at 37 or 92 °C for 3 min. EW7 untreated cells were cultured as monolayer for 24 h and then media were removed and replaced by control (untreated), βgal- and hIFNβ-lipofected supernatants. Cell viability was evaluated with MTS as described above.

hIFNβ antiviral biological activity

The supernatants of control (untreated), βgal- and hIFNβ-lipofected cells were collected (24 h after lipofection) and assayed by a biological method.[24] Wish cells were used as biological substrate and vesicular stomatitis virus was employed as challenge. IFN produced was always β type, as it was completely neutralized by a monoclonal anti-hIFNβ-neutralizing antibody kindly provided by BioSidus.

Statistics

Results were expressed as mean ± s.e.m. (*n*: number of experiments corresponding to independent assays). Differences between groups were determined by analysis of variance.

RESULTS AND DISCUSSION

rhIFNβ displayed a stronger cytotoxic effect than rhIFNα

Human cell lines derived from different kinds of tumors (EW7, COH: ES; M8: melanoma; MCF7: mammary adenocarcinoma; HT-29: colon adenocarcinoma) were *in vitro* incubated with 3 consecutive daily pulses of fixed concentrations (1–10 000 IU ml^{-1}) of rhIFNα (Figure 1a) or rhIFNβ (Figure 1b). The added recombinant IFN

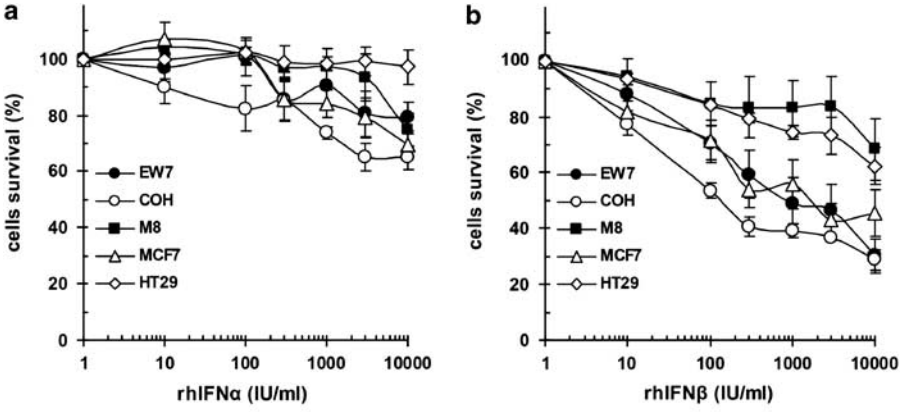

c

-	Lipofection efficiency (%)	Cytokine production (IU ml^{-1})	IC_{50} of recombinant proteins (IU ml^{-1})	
Cell line	βgal marker	hIFNβ	rhIFNα	rhIFNβ
EW7	1.0	1797±182	>10000	800
COH	1.0	1083±126	>10000	140
M8	2.5	2840±350	>10000	>10000
MCF7	18.0	3109±413	>10000	1700
HT-29	4.0	1645±078	>10000	>10000

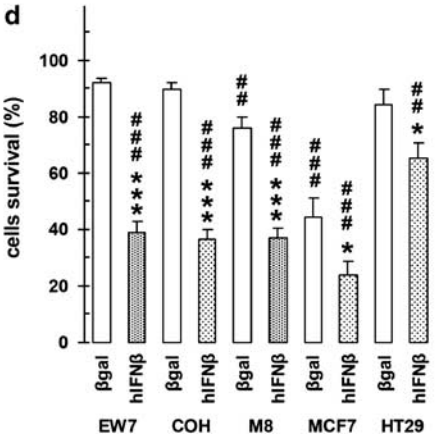

Figure 1. Cytotoxic effects of exogenously added interferon (IFN) recombinant proteins (**a**–**c**) or human IFNβ (hIFNβ) transferred gene (**d**) on tumor cell monolayers and lipofection, and gene expression efficiencies (**c**). (**a**, **b**) Cell monolayers were grown in the presence of increasing concentrations of recombinant proteins (rhIFNα or rhIFNβ) as indicated and cell viability was quantified by MTS at day 5 as described in the Materials and methods. Results were expressed as percentage of viable cells with respect to untreated control (100%) as means ± s.e.m; $n \geqslant 5$. (**c**) Lipofection efficiencies (% of X-GAL (5-bromo-4-chloro-3-indolyl β-D-galactopyranoside) staining) and hIFNβ biological activity in supernatant media were evaluated as described in the Materials and methods. (**d**) Transiently β-galactosidase (βgal)- or hIFNβ-lipofected cells were cultured as monolayers and cell viability was quantified by MTS at day 5 as described in the Materials and methods. Results are expressed as means ± s.e.m of indicated independent experiments. EW7: $n \geqslant 38$, COH: $n \geqslant 23$, M8: $n \geqslant 26$; MCF7: $n \geqslant 16$, HT-29: $n \geqslant 12$. $^{***}P < 0.001$, $^{*}P < 0.05$ with respect to βgal; $^{\#\#\#}P < 0.001$ and $^{\#\#}P < 0.01$ with respect to control.

produced a concentration-dependent inhibition of proliferation, with the exception of HT-29 that resulted refractory to rhIFNα. It is noteworthy that the cytotoxic effect caused by rhIFNβ was always higher than that caused by the equivalent amount of rhIFNα. The maximal rhIFNα inhibition (between 30 and 20%) of EW7, COH, M8 and MCF7 was significant ($P<0.01$) only at the maximal tested concentration (10 000 IU ml^{-1}). At the tested range, rhIFNα did not reach the half-maximal inhibitory concentration (IC_{50}) in any tumor cell line, and hence the IC_{50}s for this protein could not be established. On the other hand, COH cells started to be significantly sensitive to rhIFNβ from 10 IU ml^{-1} ($P<0.01$), and EW7 and MCF7 did so from 100 IU ml^{-1} ($P<0.01$), whereas M8 was sensitive only at 10 000 IU ml^{-1} ($P<0.05$). As defined by the rhIFNβ IC_{50}s, COH, EW7 and MCF7 cells resulted, respectively, at least 70-, 12- and 6-fold more sensitive to rhIFNβ than to rhIFNα. M8 and HT-29 cell survival curves always appeared rightward from the other ones, indicating a significant resistance to hIFNβ and precluding the calculation of the IC_{50}s (Figure 1c).

Lipofection with hIFNβ gene showed a significant cytotoxic effect

To establish the feasibility of a nonviral gene therapy achieved by lipoplexes carrying the hIFNβ gene, we lipofected the above-mentioned cell lines. As shown in Figure 1d, viability of βgal-expressing EW7, COH, M8 and HT-29 ranged 75–95%, whereas in the case of MCF-7 it was only 45%, possibly because lipoplex treatment stimulated the expression and release of hIFNβ.[25] The transfer of hIFNβ gene produced an additional strong cell viability inhibition (50%) in EW7, COH, MCF7 and M8. HT-29 resulted only moderately sensitive to hIFNβ gene (30%). Taking into account the low lipofection efficiencies of ES, melanoma and colon adenocarcinoma cells (Figure 1c), this outcome result was very encouraging.

As displayed in Figure 1c, the levels of biologically active hIFNβ protein secreted by lipofected cells 24 h after gene transfer varied from ~1000 to 3000 UI ml^{-1} per day, reflecting the balance between protein synthesis/secretion and degradation in the culture medium. It is worth noting that these levels did not correlate with cytotoxic effects, probably because of: (1) the different susceptibility of each tumor cell line, or (2) the effect of extracellular rhIFNβ could be spare or redundant with respect to the endogenously synthesized cytokine.

Highly sensitive COH and EW7 cells and poorly sensitive HT-29 cells displayed no significant differences between hIFNβ-lipofected gene and the exogenously added recombinant protein (10 000 IU ml^{-1}). Conversely, the cytotoxic effects of the lipofected hIFNβ gene resulted significantly higher in M8 and MCF7 than those of 3 daily additions of exogenously added rhIFNβ at the concentration produced by the lipofected cells (Figures 1b–d). This indicates that hIFNβ gene lipofection might have a broader spectrum of cytotoxic effects than those triggered by exogenous recombinant hIFNβ protein.

Lipofected hIFNβ gene enhanced the fraction of hypodiploid sub G_1 apoptotic cells

To get a deeper insight on the mechanisms involved in the effects of hIFNβ lipofection, we analyzed hIFNβ-lipofected EW7 cells by flow cytometry (Figures 2a–e). EW7 cells were not sensitive to βgal lipofection, displaying the typical cell cycle peaks G_0/G_1, S and G_2/M (like nonlipofected control cells: Figure 2e) and a slight increase in the sub-G_1 apoptotic region (from 3 to 9% at day 5). Conversely, from day 1 after lipofection, hIFNβ gene increased the fraction of G_0/G_1, S, G_2/M and hyperdiploid cell populations. After 5 days, 87% of the total hIFNβ-lipofected cells accumulated in the hypodiploid sub-G_1 apoptotic region, whereas the fraction of cycling and hyperdiploid cell populations reduced drastically.

On the other hand, hIFNβ-induced DNA damage was confirmed by agarose gel electrophoresis of extracted genomic DNA (Figure 2f). A smear of degraded DNA clearly appeared from 96 to 120 h after initiation of treatment, with no evidence of a nucleosomal ladder, probably because of the increase of oxidant species.[26]

Lipofected hIFNβ gene induced distorted cell phenotypes

By means of hematoxylin and eosin staining (Figure 3), all hIFNβ-lipofected cell lines displayed significant morphological changes like cell volume increase (EW7), nuclear fragmentation (EW7), cytoplasmic vacuolization (M8) and condensed and pycnotic nuclei (all). MCF7 resulted particularly sensitive, showing substantial swelling after unspecific lipofection with βgal gene. Conversely, HT-29 displayed some degree of swelling after lipofection with βgal gene, without the concomitant cytoxicity.

In the cases of hIFNβ-lipofected EW7 and MCF7 cells, the presence of multinucleated giant cells was congruent with hyperdiploid apoptotic cells from the flow cytometry patterns (Figures 2 and 3).

Lipofected hIFNβ gene efficiently drove cells to death through necrosis or apoptosis

Double staining with acridine orange/ethidium bromide[27] allowed the observation of apoptotic/necrotic events following lipofection with βgal and hIFNβ genes. Cell membrane is permeable to acridine orange, leading to a homogeneous green cell staining. Ethidium bromide enters only in dying or dead cells because of the disruption in the plasmatic membrane integrity and, consequently, the compact chromatin becomes red-stained. As shown in Figure 4a, control and βgal-lipofected EW7, M8 and MCF7 mostly appeared as green-stained healthy cells. Lipofection with hIFNβ increased the number of apoptotic/necrotic events as evidenced by the increase of red-stained nuclei. In EW7, this effect, which was not detectable at 24 h, became significant between 72 and 120 h after lipofection. During this process, condensed chromatin appeared in EW7 apoptotic cells as well as red swollen necrotic cells (data not shown). At 120 h after lipofection, M8 displayed clear images of apoptotic events with a significant reduction of total cell number. MCF7 significantly increased the fraction of damaged cells distributed between apoptotic and necrotic events.

As derived from counting of ethidium bromide-stained cells 5 days after gene transfer, 87% of hIFNβ-lipofected EW7 cells appeared involved in apoptosis/necrosis as compared with only 9% of βgal-lipofected cells. In the lipofection-sensitive MCF7 cells, ~20% of βgal- and 50% of hIFNβ-lipofected cells were involved in apoptosis/necrosis pathways. Nearly 30% of M8 cells (quite resistant to rhIFNβ protein) were involved in apoptosis/necrosis as compared with only 8% of βgal-lipofected cells. Control unlipofected cells displayed a basal rate of apoptosis/necrosis ranging 1–3% under our culture conditions.

Lipofected hIFNβ gene engaged the p53 tumor-suppressor pathway

Interestingly, IFNβ expression has also been associated with upregulation of tumor-suppressor gene p53, a central regulator of the senescence response.[28] This factor plays a pivotal role in growth regulation and cell death under stress conditions. The p53 tumor-suppressor pathway is activated when the redox balance is modified, and its specific binding to DNA activates target genes.[29]

As mentioned above, hIFNβ gene transfer blocked the cell cycle progression and triggered apoptosis (Figures 2 and 4a). In EW7 at 48 h after lipofection (Figure 4b), specific immunofluorescence evidenced a significant increase of nuclear and total p53 as confirmed by western blot (Figure 4b, central inset). Western bands displayed 85% stronger expression of p53 triggered by hIFNβ with respect to βgal-lipofection (quantified with ImageJ

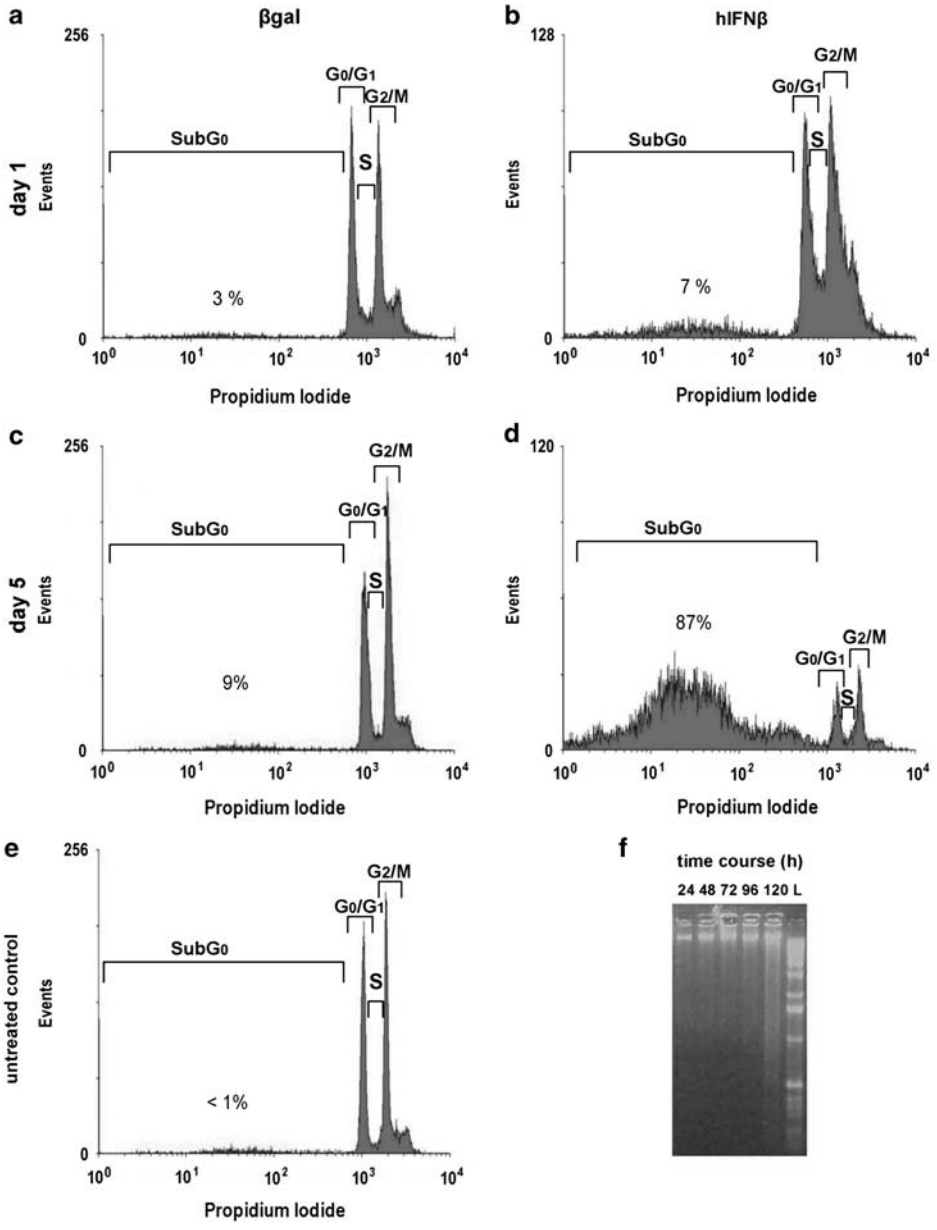

Figure 2. Flow cytometry analysis (**a**–**e**) and DNA fragmentation (**f**). EW7 cells untreated (**e**), β-galactosidase (βgal; **a**, **c**) and human interferon-β (hIFNβ; **b**, **d**) lipofected growing in monolayers for 1 or 5 days as indicated were subjected to cytometric analysis as described in the Materials and methods. (**f**) hIFNβ-lipofected EW7 cells were cultured for the indicated times, and genomic DNA integrity was analyzed by agarose gel electrophoresis as described in the Materials and methods. L: 1 Kb DNA ladder as size markers.

1.45s; NIH, software). The basal p53 levels of untreated controls were barely detected (~5% of those produced βgal lipofection). The appearance of cytoplasmic discrete dots (Figure 4b, right inset), possibly because of a mitochondrial translocation of p53, is noteworthy. Both phenomena were reported as related to oxidative stress.[30]

Lipofected hIFNβ gene depolarized the mitochondrial membrane

In general, cancer cells display a basal hyperpolarization of the mitochondrial membrane that confers them a certain degree of resistance.[31] As it has been described in Figure 1c, M8 resulted resistant to rhIFNβ protein compared with EW7 (IC_{50} >10 000 vs IC_{50}: 800 IU ml^{-1}, respectively), whereas both cell lines resulted sensitive to hIFNβ gene. One of the reasons of this difference may be because of the fact that only hIFNβ gene depolarized mitochondrial membrane in M8 (Figure 4c), thus reverting the basal hyperpolarization displayed by this resistant cell line. On the other hand, both rhIFNβ protein and hIFNβ gene decreased the mitochondrial potential in EW7, justifying the high sensitivity of this ES cell line.

Early senescence induced by hIFNβ contributed to cell death

To determine the status of the cells that apparently survived the treatment with hIFNβ gene, we assayed the cellular acidic senescence-associated βgal activity (SA-βgal).[32] As shown in Figure 5b, at day 7 after lipofection with hIFNβ, 50% of EW7 cells stained for SA-βgal. But these cells comprised those that survived the treatment, ~40% of the initial cells. This means that 20% of the initial cells finally entered early senescence and only 20% remained viable.

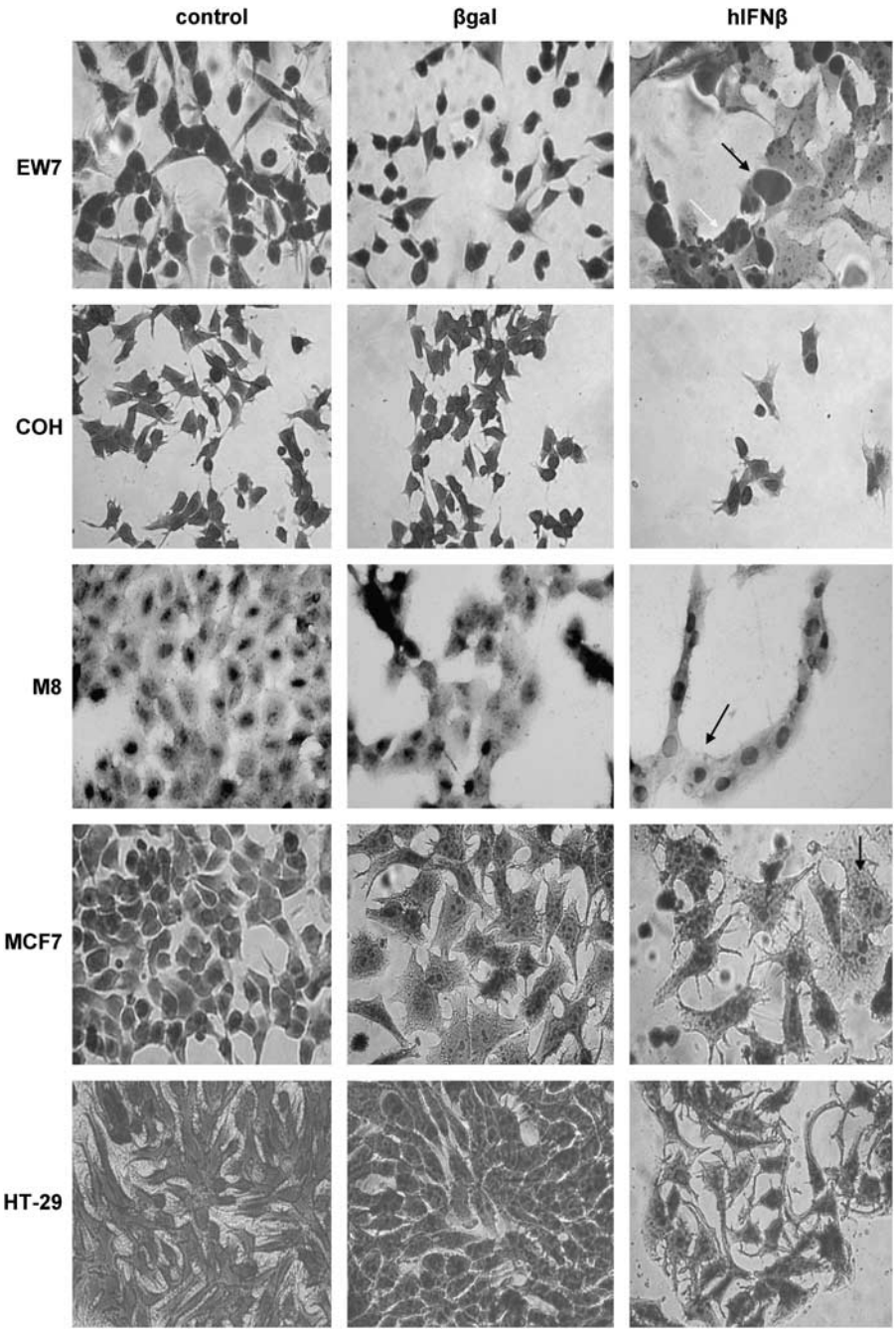

Figure 3. Hematoxylin and eosin staining of treated cells. Untreated and β-galactosidase (βgal) or human interferon-β (hIFNβ)-lipofected cells were fixed and stained as indicated in the Materials and methods (magnification $\times$ 400).

Furthermore, the addition of exogenous rhIFNβ (3 consecutive days, Figure 5a) displayed an increase of SA-βgal-positive cells proportional to the concentration, reaching at 10 000 IU ml^{-1}, values similar to those obtained by lipofection with hIFNβ.

These results indicate that early senescence would be associated specifically to hIFNβ rather than to lipofection procedure effects.

hIFNβ transgene expression displayed a remarkable bystander effect

Because IFNβ is secreted out of cells, we would expect both autocrine and paracrine effects, resulting in a very significant bystander effect. The extent of cytotoxicity due to hIFNβ gene transfer and expression (Figure 1d) widely exceeded the lipofection efficiencies (Figure 1c). In the case of EW7, only 1% of lipofected cells produced >60% of cell death, suggesting the occurrence of a strong bystander effect. This was confirmed by the fact that the dilution of hIFNβ-lipofected EW7 cells with control βgal-lipofected EW7 cells up to 50% (that actually means 0.50% of positive βgal-expressing cells) did not significantly modify the cytotoxic effect (Figure 6a). Only when the decreasing proportion of hIFNβ-lipofected cells reached 0.25%, the cytotoxicity significantly diminished ($P<0.05$). In addition, we found that hIFNβ-lipofected (but not βgal-lipofected) EW7 cell supernatant displayed cytotoxic effect when added to nontreated EW7 cells (Figure 6b). The incubation of this supernatant at 92 °C during 3 min for hIFNβ denaturation

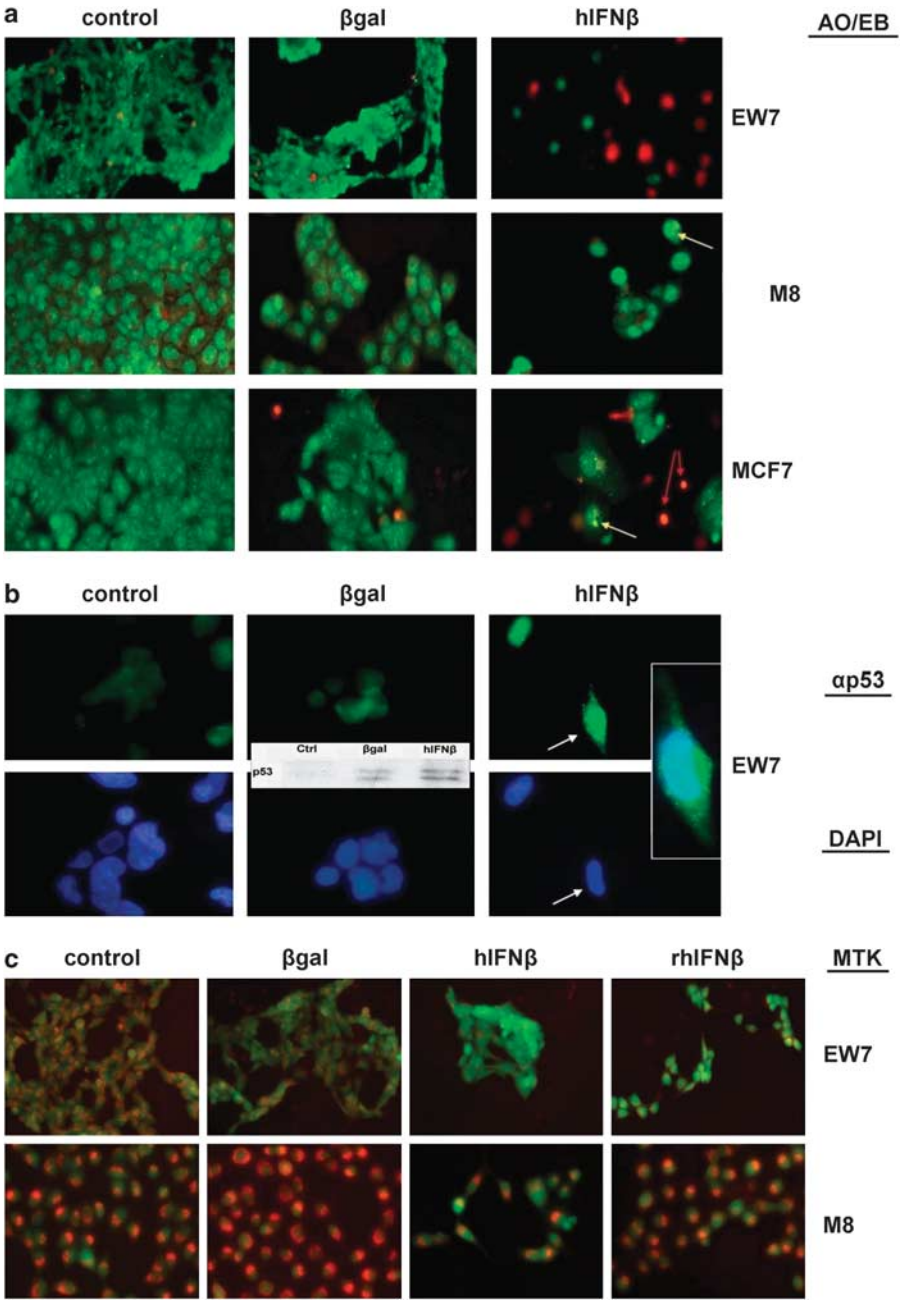

Figure 4. Detection of apoptotic cells (**a**), p53 (**b**) and mitochondrial potential (**c**) by fluorescence microscopy. (**a**) Acridine orange/ethidium bromide staining (AO/EB) of control (untreated), β-galactosidase (βgal)- and human interferon-β (hIFNβ)-lipofected cells at 120 h after lipofection was performed as described in the Materials and methods (magnification × 200). Cells stained green (viable), red (necrotic or late apoptotic) or yellow nuclei (apoptotic). Inserts display detailed chromatin condensation (M8) and fragmented nuclei (MCF7); yellow arrows indicate apoptotic processes, and red arrows indicate necrotic processes. Each experiment was performed in triplicate ($n = 3$) and generated similar morphological features. (**b**) p53 and DAPI (2-(4-amidinophenyl)-6-indolecarbamidine dihydrochloride) staining and p53 western blot of EW7 cells (αp53, DAPI). Immunocytochemistry of untreated and β-gal- or hIFN-β-lipofected cells at 120 h after lipofection incubated with p53 antibody. hIFN-β-lipofected cells present p53-positive (white arrow) nuclear and cytoplasmic staining (magnification × 400). Right inset: overlapping of both stainings. Western blot (centered inset) was performed as described in the Materials and methods. (**c**) Mitochondrial potential (MTK). Calcein/MitoTracker Red-CMXRos staining of control (untreated), βgal- and hIFNβ-lipofected or exogenously added recombinant protein (rhIFNβ; 3 times) cells was performed 120 h after treatment as described in the Materials and methods (red staining indicates conserved mitochondrial potential whereas green staining indicates viable cells; magnification × 200).

partially decreased its cytotoxicity, indicating the possible involvement of additional thermostable bystander factors (data not shown).

Even though with much higher gene transfer efficiencies, a bystander effect for adenoviral-mediated IFN-α (Ad-IFNα) was previously reported. Ad-IFNα was cytotoxic both to cancer cells that are sensitive and to those that are resistant to rhIFNα. Three different mechanisms were proposed: (1) the direct effect of hIFNα production in rhIFNα-sensitive cells; (2) the direct effect of Ad-IFNα infection and high levels of hIFNα expression in rhIFNα-resistant

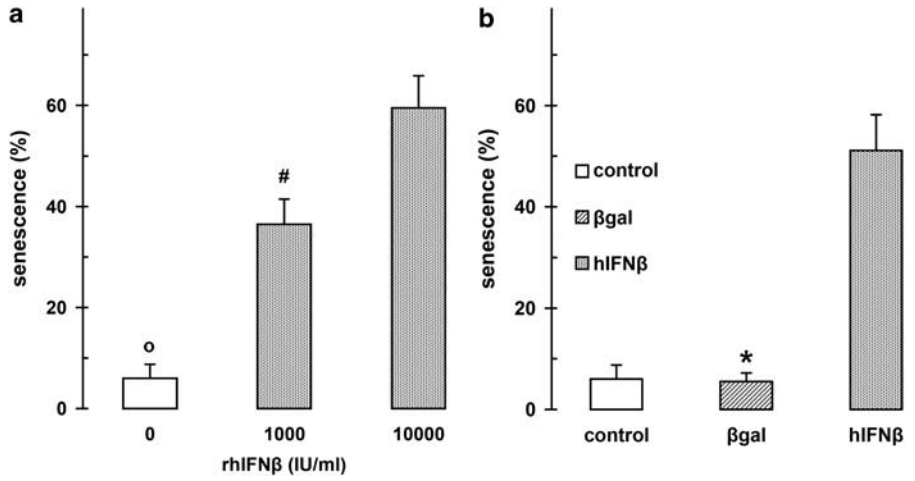

Figure 5. Induction of early senescence by added (**a**) recombinant protein (rhIFNβ) and lipofection with (**b**) human interferon-β (hIFN-β) in EW7 cells. Senescence-associated expression of β-galactosidase (gal) activity was determined as described in the Materials and methods. Results were expressed as percentage of stained cells as means ± s.e.m; $n \geqslant 4$. *$P < 0.02$ with respect to hIFNβ; #$P < 0.05$ with respect to rhIFNβ (10 000); °$P < 0.05$ with respect to rhIFNβ (1000).

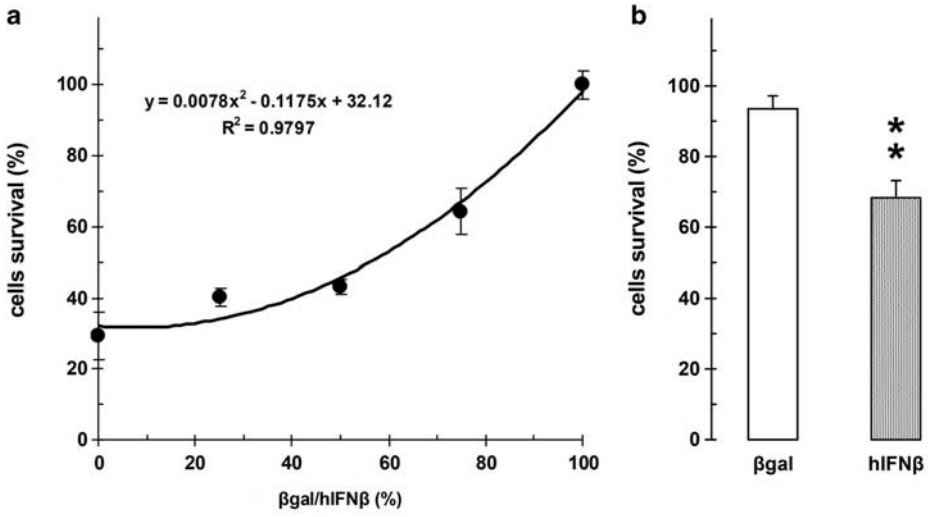

Figure 6. Bystander effect of human interferon-β (hIFNβ) lipofection on EW7 tumor cells (**a**) and of hIFNβ-lipofected cell supernatant on nontreated EW7 cells (**b**). (**a**) *In vitro* sensitivity of different combinations of hIFNβ- and β-galactosidase (βgal)-lipofected cells. Transiently hIFNβ-lipofected EW7 cells were mixed with their respective βgal-lipofected controls at proportions of 0, 25, 50, 75 and 100%. The mixtures were seeded as monolayer cultures on 96-well plates. (**b**) Sensitivity of nontreated EW7 cells to hIFNβ-lipofected cell supernatant. After 5 days, cell viability was quantified by MTS as described in the Materials and methods. Results are expressed as mean ± s.e.m of four independent experiments. **$P < 0.01$ with respect to βgal.

cancer cells; and (3) the indirect effect of the Ad-IFNα bystander factors produced.[33]

Lipofected hIFNβ gene increased the production of reactive oxygen species

In accordance with the results on the decrease of mitochondrial potential (Figure 4c), we also found that both hIFNβ gene and rhIFNβ protein increased intracellular oxidant species in EW7 (Figure 7a), whereas only hIFNβ gene did so in M8 (data not shown). These results suggest that both mitochondrial membrane depolarization and oxidative stress may be required for the antitumor IFN actions.

In addition, starting at 48 h after lipofection, hIFNβ significantly ($P < 0.02$) increased the superoxide anion (O_2^-) production by EW7 (Figure 7b). The increase of O_2^- levels could be because of alteration of mitochondrial function, inhibition of endogenous SOD or a combination of both events. Preliminary data indicated that SOD would be not only not inhibited but enhanced during the first 48 h after lipofection with hIFNβ (control = 3 IU per 10^6 cells vs hIFNβ = 22 IU per 10^6 cells). This fact would constitute an antioxidant cell response triggered by the treatment. Then, as a result of incomplete coupling of electrons with hydrated protons (H_3O^+) in the respiratory chain, mitochondrial metabolism may be the main source of O_2^-.

In addition, we evaluated whether ROOHs, which are able to cross cell membrane, were present in the extracellular media. As shown in Figure 7c, lipofection with hIFNβ gene also produced a significant increase ($P < 0.05$) in ROOHs on or after 72 h of treatment. This increase in ROOH levels could be because of a higher production or lower activity of degrading enzymes (that is, CAT) or to a combination of both events. Preliminary

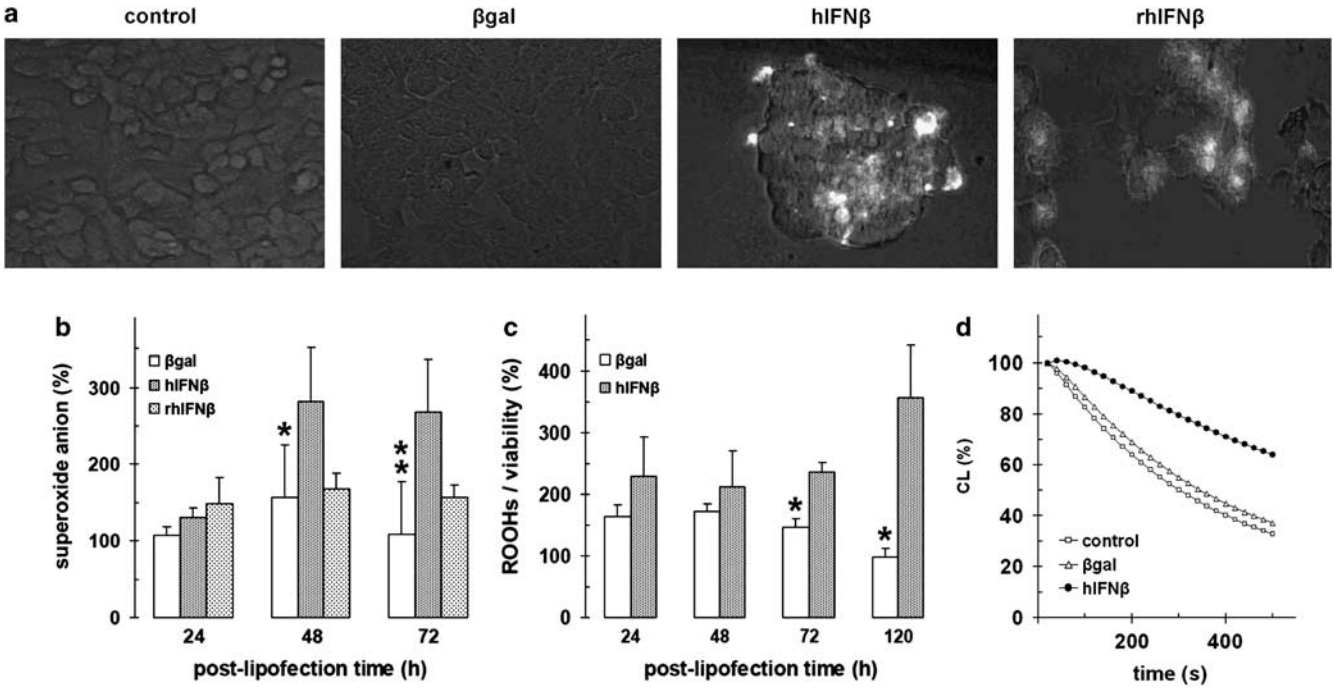

Figure 7. (**a**) Oxidative stress. Control (untreated), β-galactosidase (βgal)-lipofected, human interferon-β (hIFNβ)-lipofected or exogenously added recombinant protein (rhIFNβ; 3 times) cells were incubated with H_2DCF-DA 120 h after treatment as described in the Materials and methods. Total cells are visualized by contrast phase microscopy (magnification × 200). Each experiment was performed in triplicate ($n = 3$) and generated similar morphological features. Determination of reactive oxygen species (ROS): superoxide anion (**b**) and hydrosoluble peroxides (**c**) in hIFNβ-lipofected EW7 cells were measured as described in the Materials and methods. Decrease in cellular antioxidant capacity (**d**): Control (untreated, □), βgal (△)- and hIFNβ-lipofected (●) cells were incubated with luminol and an excess of H_2O_2. The chemoluminiscence (CL) of oxidized luminol was evaluated as described in the Materials and methods. The capacity of hIFNβ-lipofected cells to remove oxidized luminol was significantly different from control and βgal ($P < 0.05$). Results are expressed as percentages of the values obtained for untreated cells (100%) as mean ± s.e.m (**b**: $n = 4$; **c**: $n = 8$; **d**: $n = 4$). $^{**}P < 0.01$, $^{*}P < 0.05$ with respect to hIFNβ.

results demonstrated that an unspecific inhibitor of peroxidases[34] was increased in the cytosolic compartment of hIFNβ-expressing EW7 cells (data not shown). On the other hand, we found that hIFNβ gene decreased the antioxidant capacity of EW7 cells (Figure 7d).

To ascertain the involvement of oxidant species present in the extracellular media as mediators of hIFNβ-induced cell killing, we added 100 IU ml^{-1} SOD, 1000 IU ml^{-1} CAT or a combination of both enzymes to the culture media of untreated, rhIFNβ-treated or both hIFNβ- or βgal-expressing EW7 and M8 cells (Figure 8). Even though separately they showed no effects, the combination of CAT plus SOD was able to partially revert the strong cytotoxic effect of hIFNβ gene lipofection (from 50 to 25%, $P < 0.05$) and almost completely blocked the low cytotoxic effect of 3000 IU ml^{-1} rhIFNβ (from 30 to 10%; $P < 0.01$) in M8. In the case of ES cell line, we found that the strong cytotoxic effect of 3000 IU ml^{-1} rhIFNβ was partially reverted (from 75 to 60%, $P < 0.05$) by the combination of the antioxidant enzymes. No significant effects were observed on hIFNβ-lipofected EW7 cells.

CONCLUSION

A better understanding of the antitumor mechanisms and the identification of the factors responsible for resistance to IFNβ gene lipofection could lead to its improved use in malignant and other diseases.

As already reported,[2,14] here we confirmed that the cytotoxic response induced by rhIFNβ was superior to that of rhIFNα on all tested cell lines. Most relevant to the present work was the demonstration of that hIFNβ gene lipofection could constitute an approach that produces an equivalent or higher effect than elevated doses of the exogenously applied protein rhIFNβ (Figure 1).

As intracellular hIFNβ RNA concentration was suggested as positive regulator of endogenous hIFNβ antitumor activity,[35] a more complex mechanism of action would be involved in cells expressing hIFNβ and their neighbors than in cells receiving it exogenously.

Even though lipofected hIFNβ gene drove 20% of tumor cells to early senescence, the dramatic reduction in the viability of EW7, COH, M8 and MCF7 cells appeared to be primarily the result of apoptotic and necrotic events (Figures 2 and 4). After 5 days of hIFNβ gene lipofection, 87% of the total EW7 cells accumulated in the hypodiploid sub-G_1 apoptotic/necrotic region (Figure 2d).

One of the main reasons for the success of hIFNβ gene treatment would be the strong bystander effect promoted by this cytokine. This effect eliminated up to 60% of the ES cells, even though only 1% of them expressed measurable amounts of transgene. The high effectiveness of transgenic hIFNβ agrees with previous reports demonstrating that as few as 1% of implanted cells (*ex vivo* IFNβ gene transduced by a replication-defective adenovirus) blocked *in vivo* tumor formation.[36] Taking into account the considerably low hIFNβ gene transfer and expression, the successful killing of such high proportion of ES cells was an unexpectedly good outcome (Figure 1). On the other hand, the other treatment that relies on the bystander effect, the suicide system HSV*tk*/GCV,[16] did not work on these cells (data not shown). This difference suggests that HSV*tk*/GCV probably requires a higher basal percentage of lipofection efficiency to work, thus proposing hIFNβ as a less limited approach in this kind of therapy. We also may argue that the main difference between both systems is the fact that hIFNβ can be secreted by the lipofected

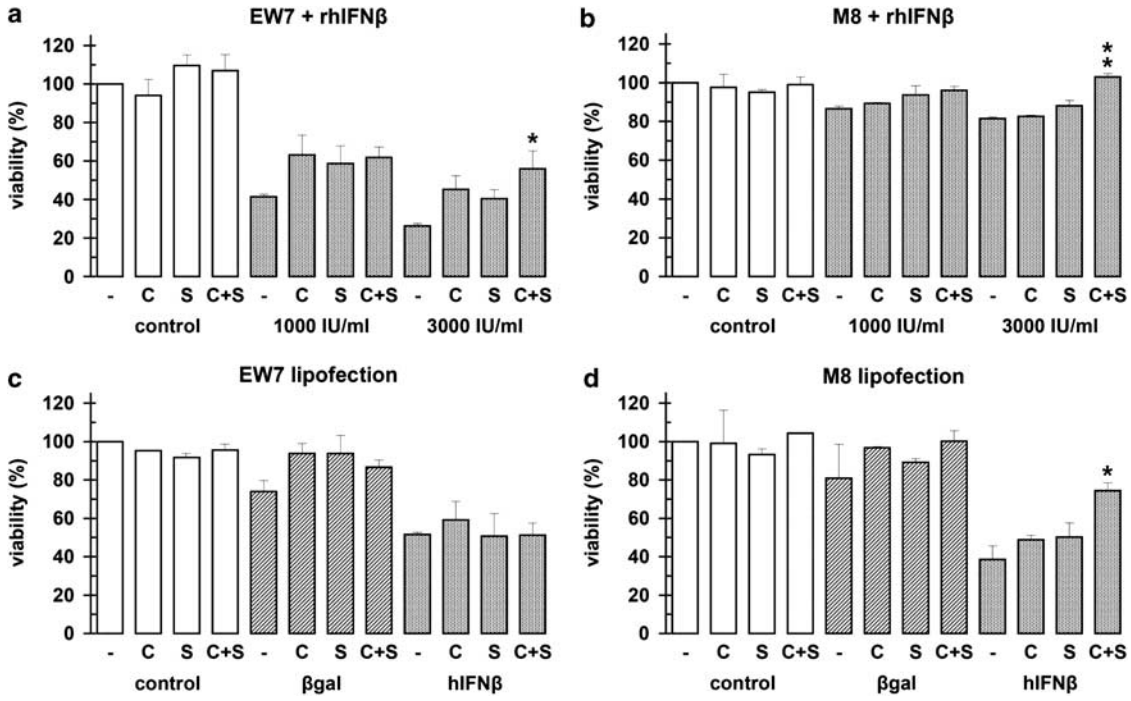

Figure 8. Addition of exogenous antioxidant enzymes. Culture medium of EW7 (**a**, **c**) and M8 (**b**, **d**) cells untreated (control), β-galactosidase (βgal) and human interferon-β (hIFNβ) (**c**, **d**) lipofected or incubated with 1000–3000 IU ml^{-1} of rhIFNβ (**a**, **b**) were supplemented with 1000 IU ml^{-1} catalase (CAT; C), 100 IU ml^{-1} superoxide dismutase (SOD; S) or a combination of both antioxidant enzymes (C + S). Cell viability was quantified by MTS at day 5 as described in the Materials and methods. Results are expressed as means ± s.e.m of four independent experiments. $^{**}P < 0.01$, $^{*}P < 0.05$ with respect to no additions.

cells and thereby reach their nonlipofected neighbors. Then, we could expect both autocrine and paracrine effects, perhaps resulting in a very significant bystander effect. Nevertheless, in the case of M8 and MCF7, the treatment with 3 daily additions of a high concentration of rhIFNβ protein produced a lower response than hIFNβ gene lipofection. Then, the powerful bystander effect of the lipofection with hIFNβ gene supports the involvement of additional cell death mediators.

In agreement with this hypothesis, we found that only hIFNβ gene significantly depolarized mitochondrial membrane in M8 cells (Figure 4c), thus reverting their basal hyperpolarization that confers them a certain degree of resistance.[31] On the other hand, both rhIFNβ protein and hIFNβ gene decreased the mitochondrial membrane potential in EW7-sensitive cell line (Figure 7a). In addition, this decrease in mitochondrial potential was simultaneous to an increase in oxidative stress caused by hIFNβ gene in both cell lines (Figure 7a and data not shown). We found an increase in superoxide anion simultaneous to a decrease in the antioxidant capacity of EW7 cells. Furthermore, we also demonstrated that the ROOHs produced by hIFNβ-lipofected EW7 cells were able to reach adjacent unmodified tumor cells, leading them to oxidative damage (Figure 7b). This phenomenon would activate amplification mechanisms allowing that few hIFNβ-lipofected cells trigger the destruction of a high proportion of bystander cells. These results agree with previous studies that reported an essential role of mitochondria in the rhIFNβ-induced cancer cell death.[37]

As displayed in Figure 1b, melanoma M8 and colon carcinoma HT-29 cell lines were highly resistant to rhIFNβ protein whereas ES EW7 and mammary adenocarcinoma MCF7 were more sensitive. This pattern significantly changed when hIFNβ gene lipofection was done (Figure 1d), making M8 as sensitive to the cytokine treatment as EW7. Whereas the recombinant protein is reaching cells from outside, the hIFNβ transgene is also being synthesized and acting from the inside. A previous report showed that a truncated hIFNβ that cannot be secreted by transfected cells was able to display biological activities similar to those of extracellular hIFNβ.[38] Thus, a different regulatory pathway could be responsible for the strong bystander effect in a context of low gene transfer efficiency and expression. Possibly, reactive oxygen species and other small pro-apoptotic molecules involved in such effects can pass or diffuse from lipofected cells to their neighbors via intercellular channels. The fact that EW7 cells appeared intimately associated with each other as cell aggregates in which single cells could not be clearly distinguished could support this hypothesis. In this context, hIFNβ protein displayed its cytotoxicity when exogenously added or secreted by neighboring cells (as demonstrated with the conditioned media). But the effect of extracellular rhIFNβ could be spare or redundant when the strong bystander effect is triggered by the endogenously synthesized cytokine. This assumption is also supported by these facts: (1) the levels of rhIFNβ in the culture medium of hIFNβ-lipofected cells (Figure 1c) did not correlate with its cytotoxic effects, and (2) the combination of the antioxidant enzymes (SOD + CAT) was able to partially revert the strong cytotoxic effect of 3000 IU ml^{-1} rhIFNβ protein, but not the effect of hIFNβ lipofection in EW7 cells.

These data, together with the (1) high number of cells with degraded DNA (Figures 2d and f), and (2) the upregulation (Figure 4b) and possible mitochondrial translocation of the tumor-suppressor gene p53, strongly emphasize the role of reactive oxygen species as mediators of hIFNβ lipofection bystander effects. This situation may drastically differ from the mechanism of exogenously added rhIFNβ, which depended on tumor cell features. In this study, hIFNβ gene resulted highly more effective than rhIFNβ, in particular when cells displayed a resistance phenotype, as it was found for M8.

It is also worth pointing out that our *in vitro* system does not include any of the immune mechanisms that could provide

additional antitumor activity. Then, our findings strongly support the hIFNβ gene transfer as a very promising strategy for cancer treatment.

CONFLICT OF INTEREST

The authors declare no conflict of interest.

ACKNOWLEDGEMENTS

We thank Dr Juana Wietzerbin for EW7 and COH cells, and Ana Bihary and Graciela Zenobi for technical assistance. This study was partially supported by grants from ANPCYT/FONCYT (PICT 2002-12084 and PICT 2007-00539) and UBA (PID-UBACYT-2008/2010-M027). GCG and LMEF are investigators, and MSV and MLG-C are fellows of the Consejo Nacional de Investigaciones Científicas y Técnicas (CONICET, Argentina).

REFERENCES

1 Belardelli F, Ferrantini M, Proietti E, Kirkwood JM. Interferon-alpha in tumor immunity and immunotherapy. *Cytokine Growth Factor Rev* 2002; **13**: 119–134.
2 Johns TG, Mackay IR, Callister KA, Hertzog PJ, Devenish RJ, Linnane AW. Antiproliferative potencies of interferons on melanoma cell lines and xenografts: higher efficacy of interferon beta. *J Natl Cancer Inst* 1992; **84**: 1185–1190.
3 Yoshida J, Mizuno M, Wakabayashi T. Interferon-β gene therapy for cancer: basic research to clinical application. *Cancer Sci* 2004; **95**: 858–865.
4 Matsumoto K, Kubo H, Murata H, Uhara H, Takata M, Shibata S *et al.* A pilot study of human interferon beta gene therapy for patients with advanced melanoma by *in vivo* transduction using cationic liposomes. *Jpn J Clin Oncol* 2008; **38**: 849–856.
5 Atzpodien J, Neuber K, Kamanabrou D, Fluck M, Brocker EB, Neumann C *et al.* Combination chemotherapy with or without s.c. IL-2 and IFN-alpha: results of a prospectively randomized trial of the Cooperative Advanced Malignant Melanoma Chemoimmunotherapy Group (ACIMM). *Br J Cancer* 2002; **86**: 179–184.
6 Salmon P, Le Cotonnec JY, Galazka A, Abdul-Ahad A, Darragh A. Pharmacokinetics and pharmacodynamics of recombinant human interferon-beta in healthy male volunteers. *J Interferon Cytokine Res* 1996; **16**: 759–764.
7 Tada H, Maron DJ, Choi EA, Barsoum J, Lei H, Xie Q *et al.* Systemic IFN-beta gene therapy results in long-term survival in mice with established colorectal liver metastases. *J Clin Invest* 2001; **108**: 83–95.
8 Sterman DH, Recio A, Haas AR, Vachani A, Katz SI, Gillespie CT *et al.* A phase I trial of repeated intrapleural adenoviral-mediated interferon-beta gene transfer for mesothelioma and metastatic pleural effusions. *Mol Ther* 2010; **18**: 852–860.
9 Meyer O, Schughart K, Pavirani A, Kolbe HV. Multiple systemic expression of human interferon-beta in mice can be achieved upon repeated administration of optimized pcTG90-lipoplex. *Gene Therapy* 2000; **7**: 1606–1611.
10 Finocchiaro LME, Glikin GC. Cytokine-enhanced vaccine and suicide gene therapy as surgery adjuvant treatments for spontaneous canine melanoma. *Gene Therapy* 2008; **15**: 267–276.
11 Finocchiaro LME, Villaverde MS, Gil Cardeza ML, Riveros MD, Glikin GC. Cytokine-enhanced vaccine and interferon-β plus suicide gene as combined therapy for spontaneous canine sarcomas. *Res Vet Sci* 2011; **91**: 230–234.
12 Chiocca EA, Smith KM, McKinney B, Palmer CA, Rosenfeld S, Lillehei K *et al.* A phase I trial of Ad.hIFN-beta gene therapy for glioma. *Mol Ther* 2008; **16**: 618–626.
13 Wakabayashi T, Natsume A, Hashizume Y, Fujii M, Mizuno M, Yoshida J. A phase I clinical trial of interferon-beta gene therapy for high-grade glioma: novel findings from gene expression profiling and autopsy. *J Gene Med* 2008; **10**: 329–339.
14 Sancéau J, Poupon MF, Delattre O, Sastre-Garau X, Wietzerbin J. Strong inhibition of Ewing tumor xenograft growth by combination of human interferon-alpha or interferon-beta with ifosfamide. *Oncogene* 2002; **21**: 7700–7709.
15 Gnjatic S, Cai Z, Viguier M, Chouaib S, Guillet JG, Choppin J. Accumulation of the p53 protein allows recognition by human CTL of a wild-type p53 epitope presented by breast carcinomas and melanomas. *J Immunol* 1998; **160**: 328–333.
16 Gil Cardeza ML, Villaverde MS, Fiszman GL, Altamirano NA, Cwirenbaum RA, Glikin GC *et al.* Suicide gene therapy on spontaneous canine melanoma: correlations between *in vivo* tumors and their derived multicell spheroids *in vitro*. *Gene Therapy* 2010; **17**: 26–36.
17 Dimri GP, Lee X, Basile G, Acosta M, Scott G, Roskelley C *et al.* A biomarker that identifies senescent human cells in culture and in aging skin *in vivo*. *Proc Natl Acad Sci USA* 1995; **92**: 9363–9367.
18 Brown SV, Hosking P, Li J, Williams N. ATP synthase is responsible for maintaining mitochondrial membrane potential in bloodstream form Trypanosoma brucei. *Eukaryot Cell* 2006; **5**: 45–53.
19 Dong X, Mattingly CA, Tseng MT, Cho MJ, Liu Y, Adams VR *et al.* Doxorubicin and paclitaxel-loaded lipid-based nanoparticles overcome multidrug resistance by inhibiting P-glycoprotein and depleting ATP. *Cancer Res* 2009; **69**: 3918–3926.
20 Cheng JC, Klausen C, Leung PC. Hydrogen peroxide mediates EGF-induced down-regulation of E-cadherin expression via p38 MAPK and Snail in human ovarian cancer cells. *Mol Endocrinol* 2010; **24**: 1569–1580.
21 Lejeune D, Hasanuzzaman M, Pitcock A, Francis J, Sehgal I. The superoxide scavenger TEMPOL induces urokinase receptor (uPAR) expression in human prostate cancer cells. *Mol Cancer* 2006; **5**: 21.
22 Nourooz-Zadeh J, Tajaddini-Sarmadi J, Wolff SP. Measurement of plasma hydroperoxide concentration by the ferrous oxidation-xylenol orange assay in conjunction with triphenylphosphine. *Anal Biochem* 1994; **220**: 403–409.
23 L'Haridon F, Besson-Bard A, Binda M, Serrano M, Abou-Mansour E, Balet F *et al.* A permeable cuticle is associated with the release of reactive oxygen species and induction of innate immunity. *PLoS Pathog* 2011; **7**: e1002148.
24 Kauffman MA, Sterin-Prync A, Papouchado M, González E, Vidal AJ, Grossberg SE *et al.* Immunogenicity of an interferon-beta1a product. *Int J Immunopathol Pharmacol* 2011; **24**: 499–504.
25 Li S, Wilkinson M, Xia X, David M, Xu L, Purkel-Sutton A *et al.* Induction of IFN-regulated factors and antitumoral surveillance by transfected placebo plasmid DNA. *Mol Ther* 2005; **11**: 112–119.
26 Gilloteaux J, Jamison JM, Arnold D, Neal DR, Summers JL. Morphology and DNA degeneration during autoschizic cell death in bladder carcinoma T24 cells induced by ascorbate and menadione treatment. *Anat Rec A Discov Mol Cell Evol Biol* 2006; **288**: 58–83.
27 Squier MK, Cohen JJ. Standard quantitative assays for apoptosis. *Mol Biotechnol* 2001; **19**: 305–312.
28 Ferbeyre G, de Stanchina E, Lin AW, Querido E, McCurrach ME, Hannon GJ *et al.* Oncogenic ras and p53 cooperate to induce cellular senescence. *Mol Cell Biol* 2002; **22**: 3497–3508.
29 Bykov VJ, Lambert JM, Hainaut P, Wiman KG. Mutant p53 rescue and modulation of p53 redox state. *Cell Cycle* 2009; **8**: 2509–2517.
30 Mihara M, Erster S, Zaika A, Petrenko O, Chittenden T, Pancoska P *et al.* p53 has a direct apoptogenic role at the mitochondria. *Mol Cell* 2003; **11**: 577–590.
31 Bonnet S, Archer SL, Allalunis-Turner J, Haromy A, Beaulieu C, Thompson R *et al.* A mitochondria-K+ channel axis is suppressed in cancer and its normalization promotes apoptosis and inhibits cancer growth. *Cancer Cell* 2007; **11**: 37–51.
32 Wang Y, Blandino G, Oren M, Givol D. Induced p53 expression in lung cancer cell line promotes cell senescence and differentially modifies the cytotoxicity of anti-cancer drugs. *Oncogene* 1998; **17**: 1923–1930.
33 Zhang XQ, Yang Z, Benedict WF. Direct gene transfer of adenoviral-mediated interferon α into human bladder cancer cells but not the bystander factors produced induces endoplasmic reticulum stress-related cytotoxicity. *Cancer Gene Ther* 2011; **18**: 260–264.
34 Krawiec L, Pizarro R, Aphalo P, Cavanagh E, Pisarev M, Juvenal G *et al.* Role of peroxidase inhibition by insulin in the bovine thyroid cell proliferation mechanism. *Eur J Biochem* 2004; **271**: 2607–2614.
35 Osawa H, Mizuno M, Hatano M, Nakahara N, Tsuno T, Kuno T *et al.* Susceptibility to exogenously added interferon-beta protein depends on intracellular interferon-beta mRNA level in human glioma cells. *Cytokine* 2005; **32**: 240–245.
36 Qin XQ, Tao N, Dergay A, Moy P, Fawell S, Davis A *et al.* Interferon-beta gene therapy inhibits tumor formation and causes regression of established tumors in immune-deficient mice. *Proc Natl Acad Sci USA* 1998; **95**: 14411–14416.
37 Huang G, Chen Y, Lu H, Cao X. Coupling mitochondrial respiratory chain to cell death: an essential role of mitochondrial complex I in the interferon-beta and retinoic acid-induced cancer cell death. *Cell Death Differ* 2007; **14**: 327–337.
38 Shin-Ya M, Hirai H, Satoh E, Kishida T, Asada H, Aoki F *et al.* Intracellular interferon triggers Jak/Stat signaling cascade and induces p53-dependent antiviral protection. *Biochem Biophys Res Commun* 2005; **329**: 1139–1146.